Ingo Widmann, Leonid Dubrovinsky* and Hubert Huppertz*

Extended investigations on the pressure stability of $AlB_4O_6N:Cr^{3+}$

https://doi.org/10.1515/znb-2025-0024
Received April 16, 2025; accepted April 23, 2025;
published online May 23, 2025

Abstract: Recently, we discovered the aluminium oxonitridoborate $AlB_4O_6N:Cr^{3+}$, whose high-pressure/high-temperature synthesis could be optimized in the last months. This compound shows extraordinary luminescence properties, that closely resemble the famous compound ruby, whose luminescence is characterized by two narrow *R* emission lines close to each other. Apart from a slight blue shift, the main difference of the luminescence of the title compound is the presence of a single *R* line due to nearly perfect $[(Al/Cr)O_6]$ octahedra in the structure. Ruby plays a crucial role as gold standard for pressure calibration in diamond anvil cells by measuring the shift of one of these *R* lines with increasing pressure. However, the accuracy is limited at elevated pressure, since the two *R* lines broaden and eventually merge. Since the compound $AlB_4O_6N:Cr^{3+}$ showed only one single *R* line up to a pressure of at least 52 GPa, it could provide improved accuracy for the calibration of diamond anvil cells. This raises the question as to how the material behaves at even higher pressures. Therefore, we performed luminescence measurements of $AlB_4O_6N:Cr^{3+}$ up to 78(1) GPa in a diamond anvil cell and complemented our findings with single-crystal diffraction data (synchrotron) at elevated pressure to detect possible structural changes.

Keywords: *R* line; oxonitridoborate; high-pressure; diamond anvil cell; luminescence

***Corresponding authors: Leonid Dubrovinsky**, Bayerisches Geoinstitut, Universität Bayreuth, 95440 Bayreuth, Germany,
E-mail: Leonid.Dubrovinsky@uni-bayreuth.de. https://orcid.org/0000-0002-3717-7585; and **Hubert Huppertz**, Department of General, Inorganic and Theoretical Chemistry, University of Innsbruck, Innrain 80–82, 6020 Innsbruck, Austria, E-mail: Hubert.Huppertz@uibk.ac.at. https://orcid.org/0000-0002-2098-6087
Ingo Widmann, Department of General, Inorganic and Theoretical Chemistry, University of Innsbruck, Innrain 80–82, 6020 Innsbruck, Austria. https://orcid.org/0009-0009-8252-9891

1 Introduction

Research under static ultra-high pressure can be carried out in diamond anvil cells (DAC), which consist of two opposing diamonds with flattened tips, allowing samples to be squeezed between them.[1] DACs are crucial in studying material properties under extreme conditions, offering insights into phase transitions, chemical reactions, and material behavior under immense pressure.[1] The tremendous opportunities offered by diamond anvil cells were shown by Dubrovinskaia & Dubrovinsky et al. in 2016, who investigated materials at the (to the best of our knowledge) highest ever reached pressure of 1 TPa with DACs in a special setup.[2] Pressure inside the DAC has to be estimated by calibration, for which the ruby fluorescence method has become the mainly performed method for decades[1] and still is the state-of-the-art calibrating technique in DACs up to a pressure of ca. 100 GPa.[3–5] This calibration method was introduced in 1972 by Forman et al.[6] and is based on a shift of the *R* lines of Cr^{3+}-doped Al_2O_3 under hydrostatic pressure and a broadening of these lines if the ruby experiences nonhydrostatic stresses.[6] Further optimizations by Barnett et al. made this technique very rapid, convenient, and applicable for routine pressure measurements.[7] A tiny piece of ruby is placed inside the DAC along with the sample, and the luminescence is excited by strong light (e.g. a laser).[1] The resulting *R* lines are usually at around 693 nm (ambient pressure) with an energy separation of only around 29 cm^{-1}.[8] However, this close proximity of these two *R* lines restricts its technical utility as reference material for pressure calibration at elevated pressures, because of broadening and merging of the lines. Therefore, any enhancement of these luminescence characteristics while maintaining the benefits of high brightness at high temperature and pressure conditions for Cr^{3+} in a stable inorganic host material would be highly desirable. In 2024 Widmann et al. developed the promising compound $AlB_4O_6N:Cr^{3+}$ (see Figure 1),[9] which revealed extraordinary luminescence properties, low thermal expansion, high thermal stability and hardness suitable for multifunctional applications. In particular, $AlB_4O_6N:Cr^{3+}$ features an almost undistorted octahedral symmetry of the Al^{3+} sites, which leads to a single *R* line at 683 nm in contrast to the two *R* lines of ruby. Up to now, $AlB_4O_6N:Cr^{3+}$ was investigated up to a pressure of 52 GPa and fulfilled in this pressure range the

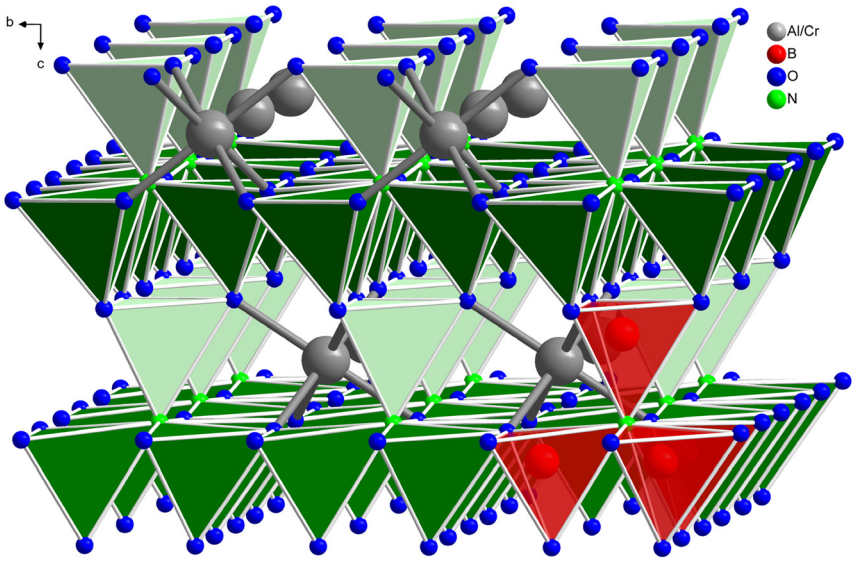

Figure 1: Crystal structure of MB_4O_6N (M = Al, Al/Cr, Cr)[9,10] in viewing direction [$\bar{1}$00]. As representative, one [$N(BO_3)_4$] building unit is colored in red, which is crystallographically identical to the green ones. Tetrahedra with a B1 atom in their centers are colored in dark green, those with a B2 in mint.

main criteria for a possible luminescent pressure sensor for more precise pressure measurements based on the presence of one single R line.

Due to these promising results, we decided to extend the investigations of $AlB_4O_6N:Cr^{3+}$ to pressures above 52 GPa. The new ultra-high pressure results were achieved with fluorescence measurements of $AlB_4O_6N:Cr^{3+}$ and ruby inside a diamond anvil cell, complemented by single-crystal measurements (synchrotron data) at elevated pressures to reveal possible structural changes. The published high-pressure/high-temperature approach for the synthesis of $AlB_4O_6N:Cr^{3+}$ was greatly improved as also reported in this paper.

2 Experimental procedures

2.1 Synthesis

For the high-pressure synthesis of $AlB_4O_6N:Cr^{3+}$ (0.7 mol% Cr^{3+}), the starting materials α-Al_2O_3 (99.99 %, Sinochem Hebei Corporation, Shijiazhuang, China), H_3BO_3 (≥99.8 %, Carl Roth GmbH & Co. KG, Karlsruhe, Germany), h-BN (≥99 %, Strem Chemicals, Newburyport, Massachusetts, U.S.), and Cr_2O_3 (99 %, Merck KGaA, Darmstadt, Germany) were weighed in (atomic ratio 1:5:5:0.00667) and the mixture ground in an agate mortar. Attempted syntheses with a stoichiometric ratio of 1:6:2 (but without Cr^{3+}) did not lead to the title compound. The starting mixture was encapsulated in platinum foil (0.027 mm, 99.9 %, Chem-Pur, Karlsruhe, Germany) with a small hole for exchange of potential volatile species. This capsule was placed in a crucible, closed with a lid (both h-BN, HeBoSint, P100, Henze Boron Nitride Products AG, Kempten, Germany), and centered in an octahedral pressure cell of an "18/11" assembly. For resistance heating, a graphite oven (FE 254, Schunk Group GmbH, Vienna, Austria) was incorporated. The assembly was placed in the center of eight beveled tungsten carbide cubes (HA–7 %Co, Hawedia, Marklkofen, Germany). The synthesis was performed under quasi-hydrostatic pressure conditions in a modified Walker-type multianvil apparatus (mavo press LPR 1000-400/50, Max Voggenreiter GmbH, Mainleus, Germany). A more detailed description of the experimental setup is published in the literature.[11–13]

The maximum pressure of 6 GPa was reached within 200 min, the maximum temperature of 1,000 °C within 10 min, and both kept constant for 20 min. The temperature was then lowered to 700 °C within 30 min, before the heating was deactivated (quenching to room temperature). Finally, the assembly was decompressed to ambient pressure conditions, which lasted 720 min. The reaction product showed, as described in the literature,[9] a rosy color in visible light and a red fluorescence when excited with ultraviolet light of 365 nm.

In contrast to our already published synthesis approach,[9] the use of a platinum capsule enabled to retain a more precise stoichiometry, because the reaction with the h-BN crucible was prevented. However, initial experiments with a *closed* platinum capsule did not lead to the searched-for product and therefore, as already pointed out, the small hole for exchange of potential gases appears to be crucial indeed. Furthermore, the amount of product could be increased and the formation of impurity phases (h-BN and c-BN) could be prevented, because without a

platinum capsule the final separation of the reaction product from the BN crucible was hardly possible. Moreover, the new synthesis approach does not need nitrates as starting materials, which could also support a more precise weighed portion, due to the water-attracting properties of nitrates.

2.2 X-ray powder diffraction analysis

The reaction product was analyzed with a STOE Stadi P powder diffractometer (STOE & Cie GmbH, Darmstadt, Germany), which was equipped with a Mythen 1K microstrip detector (Dectris, Baden-Daettwil, Switzerland) and a Ge(111) monochromator. The measurement was performed with Mo$K\alpha_1$ radiation (λ = 0.7093 Å) in transmission geometry with a flat sample holder across a 2θ range of 2.0–60.5°. A Rietveld refinement[14] was performed with the program Topas 4.2[15] (see Figure 2). Lattice parameters of a = 5.0378(2) and c = 8.2401(3) Å were determined, which are in accordance with the single-crystal values a = 5.0506(2) and c = 8.2497(3) Å for $Al_{0.97}Cr_{0.03}B_4O_6N$ available in the literature.[9] Additional reflections could be explained by 18 wt% of the side phase $NH_4B_5O_6(OH)_4{\cdot}2H_2O$.[16] In comparison to our first synthesis attempt, the ratio of the title compound and side phases (depending on the synthesis approach *h*-BN,[17] *c*-BN[18] and HP-$NH_4B_3O_5$[19]) is in the same range, but now the amount of product could be clearly increased. In the previous variant, a lot of product had to be removed in the de-assembling process.[9]

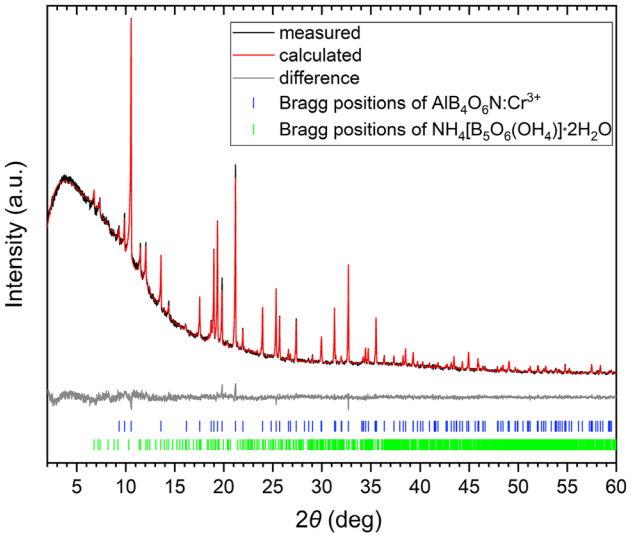

Figure 2: Rietveld refinement of the powder X-ray diffraction pattern (Mo$K\alpha_1$ radiation) of the sample with 82 wt% $AlB_4O_6N:Cr^{3+}$[9] and 18 wt% of the additional phase $NH_4B_5O_6(OH)_4{\cdot}2H_2O$.[16]

2.3 Pressure-dependent luminescence measurements

A poly-crystalline sample of $AlB_4O_6N:Cr^{3+}$ (0.7 mol% Cr^{3+}) with approximate dimensions of 7 × 7 × 3 µm^3 was loaded into a BX90 diamond anvil cell (DAC) equipped with pairs of Boehler-Almax beveled diamond anvils with culet diameters of 120 µm. The gasket was made of chemically pure Re foil indented to ≈ 15 µm thickness with a hole in the center of the indent of ≈ 60 µm in diameter. Neon (loaded as gas at ≈ 1,200 bar) was used as a pressure-transmitting medium. The local pressure was determined using a ruby standard.[20] The spectra were collected using a LabRam system equipped with an He:Ne (excitation wavelength of 632 nm) laser source. A laser power in the range of 1–15 mW was applied. Fluorescence spectra were collected with a spectrometer at a wavelength of 700 nm by means of 5 accumulations for 0.02–2 s each (depending on the intensity of the signal at different pressures).

2.4 *In situ* X-ray diffraction

In situ X-ray diffraction measurements were performed at the High-Pressure Diffraction Beamline ID15B (ESRF, Grenoble) and at P02 beamline at PETRA III (DESY, Hamburg). At ID15, an EIGER2 X CdTe 9M detector was used and a monochromatic X-ray beam (λ = 0.4099 Å) was focused on the sample with a spot area of approximately 1.5 × 1.5 µm^2. At P02 a Perkin Elmer (XRD1621) detector was used and a monochromatic X-ray beam (λ = 0.2905 Å) was focused on the sample with a spot area of approximately 2 × 3 µm^2. At each position of interest, scans of a continuous exposure with an exposure time of 2 s per frame were collected during ω rotations of ±35° of the DAC with steps of 0.5°. The resulting diffraction images were analyzed using the CrysAlis Pro[21] software suite. The Domain Auto Finder (DAFi) program was used for the search of groups of reflection's groups belonging to the individual single crystal domains.[22]

3 Results and discussion

Pressure dependent measurements of the spectral position of the *R* line of $AlB_4O_6N:Cr^{3+}$ (up to about 50(1) GPa) revealed a red shift with increasing pressure.[9] The structure analysis was performed at 52(1) GPa (single-crystal synchrotron data; inherent data is reported in this work) and showed a significant decrease of all the lattice parameters (see Table 1) and no occurrence of any phase transitions or

Table 1: Single-crystal data and structure refinement of $AlB_4O_6N:Cr^{3+}$ at 78(1) and 52(1) GPa, in comparison to published data[9] at ambient pressure (three different crystals). At 78(1) GPa a measurement at four different domains of the crystal was performed, of which one is shown as an example. Standard deviations are specified in parentheses.

	78(1) GPa (present study)	52(1) GPa (present study)	Ambient pressure (Widmann et al.[9])
Molar mass, g mol^{-1}	180.23	180.87	184.53
Crystal system		Hexagonal	
Space group		$P6_3mc$	
Single-crystal diffractometer		Four-circle diffractometer	Bruker D8 Quest
Radiation/wavelength λ, pm	Synchrotron/40.99	Synchrotron/29.05	Mo$K\alpha$/71.07
a, Å	4.704(2)	4.7934(9)	5.0506(2)
c, Å	7.669(2)	7.8427(8)	8.2497(3)
V, Å^3	146.9(2)	156.06(4)	182.25(2)
Formula units per cell Z		2	
Calculated density, g cm^{-3}	4.09	3.85	3.30
Crystal size, µm^3	7 × 7 × 3	8 × 6 × 3	80 × 40 × 20
Temperature, K	293(2)	293(2)	300(2)
Absorption coefficient, mm^{-1}	0.2	0.1	0.6
F(000), e	177	176	177
θ range, deg	3.08–18.11	2.01–17.77	4.66–37.05
Range in hkl	−4/+2 −2/+5 −11/12	−7/+6 −10/+9 −16/+15	±8; ±8; ±13
Refl. total/independent	156/112	729/337	8,135/394
R_{int}/R_σ	0.0758/0.0263	0.0231/0.0281	0.0283/0.0126
Refl. with $I > 2\ \sigma(I)$	87	292	386
Data/ref. parameters	112/25	337/29	394/29
Absorption correction		Multi-scan	
Final $R1$/w$R2$ ($I > 2\ \sigma(I)$)	0.0516/0.0558	0.0357/0.0367	0.0172/0.0466
Final $R1$/w$R2$ (all data)	0.0671/0.0570	0.0414/0.0372	0.0174/0.0467
Goodness-of-fit on F^2	3.22	1.82	1.242
Largest diff. peak/hole, e Å^{-3}	1.0/−0.9	1.2/−0.8	0.31/−0.35

decompositions.[9] In the following we discuss the results at even higher pressure.

After loading the sample into the DAC (before gas loading), the position of the single fluorescence line was measured at a wavelength of 683.7(2) nm, which is in good agreement with previous data[9] (Figure 3). Upon pressure increase in several steps, the line remained single up to 53(1) GPa and its position shifted linearly with dL/dp = 0.302(4) nm/GPa in accordance with our earlier results[9] (see Figure 3). Upon further pressure increase to 59(1) GPa, the fluorescence peak became asymmetric and clearly split into two well resolved lines upon compression above ~74 GPa (see Figure 3).

To find out the reason for the splitting, a set of diffraction data of the single crystal of the title compound inside the diamond anvil cell was measured at a synchrotron under a pressure of 78(1) GPa. This is the highest pressure at which fluorescence was collected and the splitting of the R line was already very obvious (see Figure 3). The measurement basically revealed the same structure which is also found in the literature.[9] No phase transition or decomposition occurred (see Table 2), the main difference being smaller cell parameters (see Table 1) and bond lengths (see Tables 3 and 4), due to the increased pressure, as expected. As described by Widmann et al.,[9] the splitting of the R line of Cr^{3+}-based luminescence in ruby is caused by a distortion at the octahedrally coordinated Al/Cr sites. In contrast, $AlB_4O_6N:Cr^{3+}$ shows one single R line at ambient pressure, because of nearly perfectly symmetrical [AlO_6] and [CrO_6] octahedra, whereas at 78(1) GPa a distortion seems to occur. Based on the bond lengths (see Tables 3 and 4), the difference between the M–O1 and M–O2 distances appears slightly increased, though this is still within the standard deviations. The bond angles do not show a significant change (see Table 5). Hence, a distortion could not be proven with certainty, but the single-crystal diffraction data revealed no other change in the structure and so a slight distortion within the standard deviation is the most likely explanation for the splitting of the R line. It should be mentioned that the accuracy of the

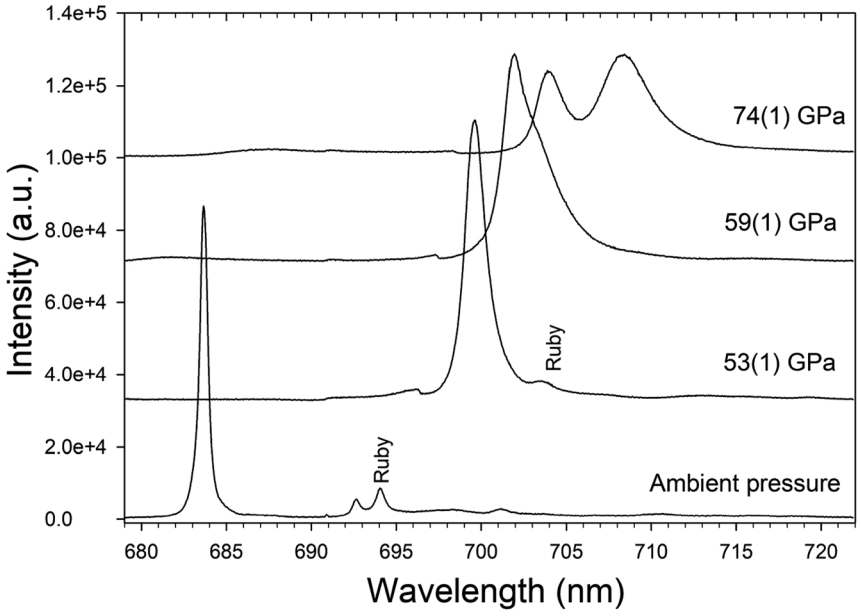

Figure 3: Examples of fluorescence spectra of $AlB_4O_6N:Cr^{3+}$ (0.7 mol% Cr^{3+}) collected upon compression using the pressure transmitting medium neon. Standard deviations are specified in parentheses.

single-crystal diffraction measurements at 78(1) GPa is quite moderate, which is expected for a material consisting of light elements compressed beyond ~75 GPa.

In contrast to ruby, which has two *R* lines, $AlB_4O_6N:Cr^{3+}$[9] has the advantage that the splitting of its single *R* line initially occurs at a pressure higher than 59(1) GPa and the

Table 2: Wyckoff positions, atomic coordinates, and site occupancy factors (s.o.f.) for $AlB_4O_6N:Cr^{3+}$ at 78(1) and 52(1) GPa (both from the present study), in comparison to published data[9] at ambient pressure (1 atm). To make the data comparable, all three data sets were standardized using the program Structure Tidy.[23] Standard deviations are specified in parentheses and are referring to the last decimal place. At 78(1) GPa a measurement at four different domains of the crystal was performed, of which one is shown exemplarily (since all these data sets are nearly similar).

Atom	Wyckoff position	*x*	*y*	*z*	s.o.f.
78(1) GPa (present study)					
Al1	2*b*	1/3	2/3	0.061(2)	0.96(3)
Cr1	2*b*	1/3	2/3	0.061(2)	0.04(3)
B1	6*c*	0.827(2)	−*x*	0.250(2)	1
B2	2*a*	0	0	0.000(3)	1
O1	6*c*	0.509(2)	−*x*	0.193(2)	1
O2	6*c*	0.841(2)	−*x*	0.431(2)	1
N1	2*a*	0	0	0.176(2)	1
52(1) GPa (present study)					
Al1	2*b*	1/3	2/3	0.0691(5)	0.98
Cr1	2*b*	1/3	2/3	0.0691(5)	0.02
B1	6*c*	0.8317(4)	−*x*	0.2566(6)	1
B2	2*a*	0	0	0.0000(7)	1
O1	6*c*	0.5065(2)	−*x*	0.2006(6)	1
O2	6*c*	0.8408(2)	−*x*	0.4373(6)	1
N1	2*a*	0	0	0.1884(6)	1
1 atm (Widmann et al.[9])					
Al1	2*b*	1/3	2/3	0.07182(7)	0.974(7)
Cr1	2*b*	1/3	2/3	0.07182(7)	0.026(7)
B1	6*c*	0.8310(2)	−*x*	0.2581(2)	1
B2	2*a*	0	0	0.0000(2)	1
O1	6*c*	0.50845(9)	−*x*	0.2047(2)	1
O2	6*c*	0.8421(2)	−*x*	0.43834(7)	1
N1	2*a*	0	0	0.1882(2)	1

Table 3: Interatomic distances (Å) in $AlB_4O_6N:Cr^{3+}$ at 78(1) and 52(1) GPa, in comparison to published data[9] at ambient pressure (standard deviations in parentheses). At 78(1) GPa a measurement at four different domains of the crystal was performed, of which one is shown as an example.

		78(1) GPa (present study)	52(1) GPa (present study)	1 atm (Widmann et al.[9])
M–	O1	1.75(2) 3×	1.769(4) 3×	1.884(2) 3×
	O2	1.74(2) 3×	1.777(4) 3×	1.8887(9) 3×
Ø*M*–O		**1.75**	**1.77**	**1.89**
B1–	O1	1.37(2) 2×	1.420(4) 2×	1.4789(8) 2×
	O2	1.39(2)	1.419(7)	1.490(2)
ØB1–O		**1.38**	**1.42**	**1.48**
B2–	O2	1.40(2) 3×	1.410(3) 3×	1.472(8) 3×
ØB2–O		**1.40**	**1.41**	**1.47**
B1–	N1	1.53(2)	1.496(3)	1.587(2)
ØB1–N1		**1.53**	**1.50**	**1.59**
B2–	N1	1.35(3)	1.477(7)	1.553(3)
ØB2–N1		**1.35**	**1.48**	**1.55**

Mean values are marked in bold.

Table 4: Interatomic distances (Å) of the [MO_6] octahedra (M = Al1, Cr1) in $AlB_4O_6N:Cr^{3+}$ at a pressure of 78(1) GPa, measured at four different domains of the single crystal inside the diamond anvil cell. Standard deviations are specified in parentheses.

		Domain 1	Domain 2	Domain 3	Domain 4
M–	O1	1.75(2) 3×	1.72(2) 3×	1.74(3) 3×	1.74(2) 3×
	O2	1.74(2) 3×	1.76(2) 3×	1.74(3) 3×	1.76(2) 3×
Ø*M*–O		**1.75**	**1.75**	**1.75**	**1.75**

Mean values are marked in bold.

Table 5: Interatomic angles (deg) in $AlB_4O_6N:Cr^{3+}$ (standard deviations in parenthesis) at 78(1) and 52(1) GPa (both from the present study), in comparison to published data[9] at ambient pressure.

	78(1) GPa (present study)	52(1) GPa (present study)	1 atm (Widmann et al.[9])
O1–*M*–O1	89.9(8) 3×	89.4(2) 3×	89.54(5) 3×
O1–*M*–$O2_{90}$	90.0(5) 6×	90.5(2) 6×	90.52(3) 6×
O2–*M*–O2	90.1(7) 3×	89.6(2) 3×	89.43(3) 3×
ØO–*M*–O_{90}	**90.0**	**90.0**	**90.0**
O1–*M*–$O2_{180}$	179.8(9) 3×	179.9(3) 3×	179.92(5) 3×
O1–B1–O1	110(2)	108.4(2)	108.3(2)
O1–B1–O2	111(2) 2×	109.6(3) 2×	109.27(8) 2×
ØO–B1–O	**111**	**109.2**	**108.9**
O1–B1–N1	109(2) 2×	110.7(2) 2×	111.20(7) 2×
O2–B1–N1	107(2)	107.9(3)	107.59(9)
ØO–B1–N1	**108**	**109.8**	**110.0**
O2–B2–O2	107(2) 3×	108.5(2) 3×	108.72(8) 3×
O2–B2–N1	112(2) 3×	110.4(3) 3×	110.21(8) 3×

Mean values are marked in bold.

peaks of the separated *R* lines can be clearly distinguished up to at least 78(1) GPa, where we terminated our measurements. Future investigations will explore the maximum pressure at which $AlB_4O_6N:Cr^{3+}$ can be compressed before its structure collapses.

4 Conclusions

The compound $AlB_4O_6N:Cr^{3+}$ has recently been prepared and characterized. It showed extraordinary luminescence properties, low thermal expansion, high thermal stability and hardness, which are all suitable for multifunctional applications.[9] Furthermore, it was shown that it fulfills the main criteria of a possible alternative luminescent pressure sensor up to at least 52 GPa, enabling more precise pressure measurements on the basis of one single *R* line.[9] Due to these intriguing findings, we extended these measurements to a pressure of 78(1) GPa, which revealed a splitting of the initial single *R* line into two separate peaks, starting above 60(1) GPa. A single-crystal structure analysis at 78(1) GPa (synchrotron data) indicated a slight distortion of the [(Al/Cr)O_6] octahedra (within the standard deviations) and revealed that no decomposition occurs under the given extreme conditions.

Acknowledgments: I.W. thanks the Vice Rectorate for Research for the grant of a doctoral fellowship at the University of Innsbruck.
Research ethics: Not applicable.
Informed consent: Not applicable.
Author contributions: The authors have accepted responsibility for the entire content of this manuscript and approved its submission.
Use of Large Language Models, AI and Machine Learning Tools: None declared.
Conflict of interest: The authors state no conflict of interest.
Research funding: None declared.
Data availability: The raw data can be obtained on request from the corresponding authors. CSD-2445735 (measurement at a pressure of 52(1) GPa) and CSD-2445736, CSD-2445760, CSD-2445765, and CSD-2445754 (measurements of the four measured domains of the single-crystal at a pressure of 78(1) GPa) contain the supplementary crystallographic data for this paper. The data can be obtained free of charge from The Cambridge Crystallographic Data Center via www.ccdc.cam.ac.uk/data_request/cif.

References

1. Jayaraman, A. *Rev. Mod. Phys.* **1983**, *55*, 65–108.

2. Dubrovinskaia, N.; Dubrovinsky, L.; Solopova, N. A.; Abakumov, A.; Turner, S.; Hanfland, M.; Bykova, E.; Bykov, M.; Prescher, C.; Prakapenka, V. B.; Petitgirard, S.; Chuvashova, I.; Gasharova, B.; Mathis, Y.-L.; Ershov, P.; Snigireva, I.; Snigirev, A. *Sci. Adv.* **2016**, *2*, e1600341.
3. Wei, Y.; Zhou, Q.; Zhang, C.; Li, L.; Li, X.; Li, F. *J. Appl. Phys.* **2024**, *135*, 105902.
4. Zhou, W.; Yin, Y.; Laniel, D.; Aslandukov, A.; Bykova, E.; Pakhomova, A.; Hanfland, M.; Poreba, T.; Mezouar, M.; Dubrovinsky, L.; Dubrovinskaia, N. *Commun. Chem.* **2024**, *7*, 209.
5. Motaln, K.; Uran, E.; Giordano, N.; Parsons, S.; Lozinsek, M. *J. Appl. Crystallogr.* **2025**, *58*, 221–226.
6. Forman, R. A.; Piermarini, G. J.; Barnett, J. D.; Block, S. *Science* **1972**, *176*, 284–285.
7. Barnett, J. D.; Block, S.; Piermarini, G. J. *Rev. Sci. Instrum.* **1973**, *44*, 1–9.
8. Maiman, T. H. *Nature* **1960**, *187*, 493–494.
9. Widmann, I.; Kinik, G.; Jähnig, M.; Glaum, R.; Schwarz, M.; Wüstefeld, C.; Johrendt, D.; Tribus, M.; Hejny, C.; Bayarjargal, L.; Dubrovinsky, L.; Heymann, G.; Suta, M.; Huppertz, H. *Adv. Funct. Mater.* **2024**, *34*, 2400054.
10. Fuchs, B.; Johrendt, D.; Bayarjargal, L.; Huppertz, H. *Angew. Chem. Int. Ed.* **2021**, *60*, 21801–21806.
11. Huppertz, H. *Z. Kristallogr.* **2004**, *219*, 330–338.
12. Walker, D.; Carpenter, M. A.; Hitch, C. M. *Am. Mineral.* **1990**, *75*, 1020–1028.
13. Walker, D. *Am. Mineral.* **1991**, *76*, 1092–1100.
14. Rietveld, H. *J. Appl. Crystallogr.* **1969**, *2*, 65–71.
15. Topas (version 4.2). *General Profile and Structure Analysis Software for Powder Diffraction Data*; Bruker AXS Inc.: Madison, Wisconsin (USA), 2009.
16. Becker, P.; Held, P.; Bohatý, L. *Cryst. Res. Technol.* **2000**, *35*, 1251–1262.
17. Hassel, O. *Nor. Geol. Tidsskr.* **1927**, *9*, 266–270.
18. Wentorf, R. H., Jr. *J. Chem. Phys.* **1957**, *26*, 956.
19. Sohr, G.; Wilhelm, D.; Vitzthum, D.; Schmitt, M. K.; Huppertz, H. *Z. Anorg. Allg. Chem.* **2014**, *640*, 2753–2758.
20. Shen, G.; Wang, Y.; Dewaele, A.; Wu, C.; Fratanduono, D. E.; Eggert, J.; Klotz, S.; Dziubek, K. F.; Loubeyre, P.; Fat'yanov, O. V.; Asimow, P. D.; Mashimo, T.; Wentzcovitch, R. M. M. *High Pressure Res.* **2020**, *40*, 299–314.
21. CrysAlis Pro Software System. *Data Collection and Processing Software*; Agilent Technologies Ltd: Yarnton, Oxfordshire (U.K.), 2014.
22. Aslandukov, A.; Aslandukov, M.; Dubrovinskaia, N.; Dubrovinsky, L. *J. Appl. Crystallogr.* **2022**, *55*, 1383–1391.
23. Gelato, L. M.; Parthé, E. *J. Appl. Crystallogr.* **1987**, *20*, 139–143.